Article

Treatment of Winery Wastewater with a Combination of Adsorption and Thermocatalytic Processes

Nuno Jorge [1,2] , **Ana R. Teixeira** [2] , **Vanessa Guimarães** [2] , **Marco S. Lucas** [2] **and José A. Peres** [2,*]

1   Escuela Internacional de Doctorado (EIDO), Campus da Auga, Campus Universitário de Ourense, Universidade de Vigo, As Lagoas, 32004 Ourense, Spain; njorge@uvigo.es
2   Centro de Química de Vila Real (CQVR), Departamento de Química, Universidade de Trás-os-Montes e Alto Douro (UTAD), Quinta de Prados, 5001-801 Vila Real, Portugal; ritamourateixeira@gmail.com (A.R.T.); guimavs@gmail.com (V.G.); mlucas@utad.pt (M.S.L.)
*   Correspondence: jperes@utad.pt

Abstract: The release of winery wastewater (WW) into the environment, without proper treatment, can cause severe problems to freshwater quality and natural fauna and flora. Therefore, in this work a treatment process was studied, combining adsorption and thermocatalytic oxidation processes. In a more specific way, it optimized the combination of activated sodium bentonite (Na-Mt) and potassium persulfate (KPS)/sodium percarbonate (SPC) as oxidant agents. With the combination of best operational conditions of adsorption ([Na-Mt] = 5.0 g/L, pH = 3.0, V = 500 mL, agitation 350 rpm, T = 298 K, t = 24 h) and thermocatalytic oxidation processes ($S_2O_8^{2-}$/H_2O_2 ratio = 1:0.25, $S_2O_8^{2-}$/H_2O_2 dosage = 0.1:0.025 (g/g), pH = 7.0, T = 343 K, agitation 350 rpm, t = 2 h), a total organic carbon, chemical oxygen demand and total polyphenols removal of 76.7, 81.4 and >99% was achieved, respectively. Finally, it was evaluated the effect of the treatment processes in the germination index (GI) of different plant seeds. A GI > 80% was achieved, showing a low phytotoxicity effect of the processes applied in the winery wastewater treatment.

Keywords: adsorption process; germination index; phenolic compounds; potassium persulfate; sulfate radicals; sodium percarbonate

1. Introduction

Portugal is a Mediterranean wine producer, with an approximated vineyard area of 194,000 ha and a wine production of 6.4 MhL in 2020. It is considered the 11th largest producer and exporter of wine worldwide [1]. To produce wine, wineries generate a significant load of residues. It is estimated that for each liter of wine produced, between 1.3 and 1.5 kg of wastes are produced. Among these, up to 75% are WW [2,3]. Most of these wastewaters result from a various number of activities which includes cleaning of tanks, washing of floors and equipment, rinsing of transfer lines, bottling facilities and filtration units [4,5]. The release of these winery wastewaters without proper treatment can cause pollution of water, degradation of soil and damage to the vegetation by odors and air emissions [6]. In addition, the discharge of the winery wastewater into the soil without treatment can alter the physicochemical properties of the ground and surface waters, by affecting color, pH and electrical conductivity from the leaching of organic and inorganic ions [7].

To avoid the negative impact of the winery wastewater in the environment, several treatments have been performed, such as coagulation–flocculation–decantation [8], microalgae [9,10], Fenton and photo-Fenton processes [2,11], sulfate radicals [12] and wet air oxidation [13]. In this work, the application of adsorption with clay was studied as a treatment for winery wastewater. A similar treatment was performed by Jorge et al. [11], who observed a high organic removal from winery wastewater by the bentonite clay. Clays and clay minerals such as montmorillonite, vermiculite, illite, kaolinite and bentonite

are widely used in petroleum industries, engineering and constructions, environmental remediation, ceramics and refractories, pharmaceuticals and agricultural sectors [14,15].

Bentonite is a 2:1 expandable montmorillonite clay and its unit layer structure consists of one Al^{3+} octahedral sheets. The modification reactions alter the surface and structural characteristics of clay by replacing the interlayer cations (e.g., Na^+, K^+, Ca^{2+}) with specific species or sites [14]. Currently, bentonite is used worldwide to prevent the formation of protein haze in wines before bottling, through a process of adsorption of proteins onto the bentonite clay [16]. However, to our knowledge, the effects of adsorption with bentonite in the phenolic composition and germination index of plants were never studied before in the treatment of winery wastewater, therefore its effects are still unknown.

Sulfate radical-based advanced oxidation processes (SR-AOPs) are another process type that can be applied for winery wastewater treatment. The SR-AOPs have attracted increasing attention due to their advantages, which include: (1) high redox potential (2.5–3.1 V), (2) working under a wide range of pH [17] and (3) a longer life time (30–40 μs vs. 20 ns) than hydroxyl radicals [18,19]. The sulfate radicals can be activated by several different techniques such as: (1) alkali activation [20,21], (2) a metal catalyzed process [22–24], (3) heat activation [25,26], (4) radiation activation [27,28], (5) activated carbon [29,30] and (6) H_2O_2-based persulfate activation [31]. In this work, the activation of sulfate radicals by addition of potassium persulfate (KPS), hydrogen peroxide (H_2O_2) and heat was used for the first time in the treatment of winery wastewater. In addition, the application of H_2O_2 in solid form as sodium percarbonate (SPC, $Na_2CO_3 \bullet 1.5H_2O_2$) was tested for the first time in WW treatment. The SPC has several advantages regarding liquid H_2O_2, such as (1) exceptional storage capability, (2) safe to handle, (3) it is a sustained-release oxidizing agent and (4) SPC and its decomposition products, such as carbon dioxide, water and a small amount of sodium carbonate, are non-toxic to microorganisms in groundwater [32].

The aim of this work is (1) to evaluate the performance of activated sodium bentonite in the adsorption process for the treatment of WW, (2) to study and optimize the thermocatalytic oxidation for the treatment of WW, (3) to evaluate the effect of combined treatment adsorption–thermocatalytic oxidation processes in the germination index of plant seeds and removal of phenolic compounds.

2. Materials and Methods

2.1. Reagents and Winery Wastewater Sampling

Activated sodium Bentonite (Na-Mt) was purchased by Angelo Coimbra & Ca., Lda (Maia, Portugal), sodium percarbonate (SPC, $Na_2CO_3 \bullet 1.5H_2O_2$) by Alfa Aesar (Massachusetts, EUA) and persulfate or potassium peroxydisulfate (KPS, $K_2S_2O_8$), by Scharlau (Sentmenat, Barcelona, Spain). NaOH and H_2SO_4 (95%) were acquired by Analar Normapur (Vila Nova de Gaia, Portugal). Deionized water was used to prepare the respective solutions. The WW was collected from a private Portuguese cellar unity located in the Douro region (Northeast of Portugal). The WW samples were stored at $-40\ ^\circ C$, and the work was performed at the University of Trás-os-Montes and Alto Douro, located in Vila Real, Portugal, latitude 41°17′9.18″ N and longitude 7°44′21.45″ W.

2.2. Analytical Technics

Different physical–chemical parameters were measured in order to characterize the WW, including the chemical oxygen demand (COD), the biological oxygen demand (BOD_5), the total organic carbon (TOC) and the total polyphenols (mg gallic acid/L). The main chemical parameters measured are shown in Table 1. The COD and BOD_5 were determined according to Standard Methods (5220D; 5210D, respectively) [33]. COD analysis was carried out in a COD reactor from HACH Co. (Loveland, CO, USA) and a HACH DR 2400 spectrophotometer (Loveland, CO, USA) was used for colorimetric measurement. Biochemical oxygen demand (BOD_5) was determined using a respirometric OxiTop® IS 12 system (WTW, Yellow Springs, OH, USA). The pH was measured by a 3510 pH meter (Jenway, Cole-Parmer, UK). The TOC content (mg C/L) was measured by a Shimadzu

TOC-L CSH analyzer (Shimadzu, Kyoto, Japan). Total polyphenols content was determined following the Folin–Ciocalteau method [34]. Hydrogen peroxide concentration was followed using titanium (IV) oxysulfate (DIN 38 402H15 method) at 410 nm, by a HACH DR 2400 spectrophotometer (Loveland, CO, USA).

Phytotoxicity tests were performed, by germination of onion, cucumber, lettuce and corn seeds (standard species recommended by the US Environmental Protection Agency, the US Food and Drug Administration and the Organization for Economic Cooperation and Development [35]) and determined by Equation (1) in accordance to Varnero et al. [36] and Tiquia and Tam [37], as follows:

$$ \text{GI}(\%) = \frac{\overline{N}_{SG,T}}{\overline{N}_{SG,B}} \times \frac{\overline{L}_{R,T}}{\overline{L}_{R,B}} \times 100 \qquad (1) $$

where GI is the germination index, $\overline{N}_{SG,T}$ is the arithmetic mean of the number of germinated seeds in each extract (wastewater), $\overline{N}_{SG,B}$ is the arithmetic mean of the number of germinated seeds on standard solution (distilled water), $\overline{L}_{R,T}$ is the mean root length in each extract (wastewater) and $\overline{L}_{R,B}$ is the mean root length in control (distilled water).

Table 1. Physical–chemical characterization of winery wastewater [38].

Parameter	Value
pH	4.0
Conductivity (μS/cm)	385
Turbidity (NTU)	1205
Total Suspended Solids (mg/L)	3910
Chemical Oxygen Demand (mg O_2/L)	9870
Biochemical Oxygen Demand (mg O_2/L)	1250
Total Organic Carbon (mg C/L)	1497
Total Polyphenols (mg gallic acid/L)	87
Ferrous Iron (mg Fe/L)	0.05
Biodegradability Index—BOD_5/COD	0.13

2.3. Phenolic and Chromatic (CIELab) Characterization

Color intensity (CI) and Hue were measured as described by the OIV method [39]; total polyphenol index (TPI) was measured using the Curvelo-Garcia method [40]; total phenols, non-flavonoids and flavonoids were determined according to Kramling and Singleton [41]. Total anthocyanins (C) were analyzed by SO_2 bleaching method, as reported by Ribéreau-Gayon et al. [42]; colored anthocyanins (CA), total pigments (TP) and polymeric pigments (PP) were determined by the method described by Somers and Evans [43] and total tannins were determined by the leucoanthocyanin (LA) method [44]. All samples were analyzed by a GENESYS^{TM} 10 Series Spectrophotometer (Thermo Fisher Scientific, Waltham, Massachusetts, USA). A Shimadzu UV-2101 spectrophotometer (Shimadzu, Kyoto, Japan) was used to record the absorption spectra of the WW samples, with a scan from a range between 380 and 770 nm, with 5 nm distance, using 1 cm path length quartz cells. Data were collected to determine a measure of *L* (lightness), *a* (redness) and *b* (yellowness) coordinates using the CIELab 1976 method. This allows reliable quantification of the overall color difference of a sample when compared to a reference sample (Blanc). Color differences can be distinguished by the human eye when the difference between ΔE_{ab} values are greater than two units, in accordance to Spagna et al. [45]. All analyses were performed in duplicate. Table 2 resumes the formulas used in this work.

Table 2. Equations for phenolic composition and chromatic (CIELab) determination [38].

Equations	Parameters	References
Color intensity (CI) CI = $A_{420} + A_{520} + A_{620}$	A_{420}—absorbance at 420 nm A_{520}—absorbance at 520 nm	OIV, [39]
Hue Hue $= \frac{A_{420}}{A_{520}}$	A_{620}—absorbance at 620 nm A_{280}—absorbance at 280 nm	OIV, [39]
Total polyphenol index (TPI) TPI = $A_{280} \times$ DF	DF-dilution factor	Curvelo-Garcia, [40]
Total phenols		Kramling and Singleton, [41]
Total phenols (mg gallic acid/L) = $\frac{A_{280}^{IPT} + 0.0243}{0.0326} \times$ DF		
Non-flavonoids		Kramling and Singleton, [41]
Non-flavonoids (mg gallic acid/L) = $\frac{A_{280}^{NF} + 0.0243}{0.0326} \times$ DF		
Flavonoids		Kramling and Singleton, [41]
Flavonoids (mg gallic acid/L) = Total phenols—Non-flavonoids		
Total anthocyanins (C) C (mg/L) = $875 \times (A_1 - A_2)$	A_1—absorbance at 520 nm A_2—absorbance at 520 nm	Ribéreau-Gayon et al. [42]
Colored anthocyanins (CA) CA (mg/L) = $(A_{520}^{no\ bisulfite} \times 10) - (A_{520}^{bisulfite} \times 10)$		Somers and Evans [43]
Total pigments (TP) TP (mg/L) = $A_{520}^{HCl} \times 10$		Somers and Evans [43]
Polymeric pigments (PP) PP (mg/L) = $A_{520}^{bisulfite} \times 10$		Somers and Evans [43]
Total tannins (L.A.) L.A. (g/L) = $19.33 \times (D_2 - D_1)$	D_1 / D_2 absorbance at 550 nm	Ribéreau-Gayon and Stonestreet [44]
CIELab $\Delta L = L_1 - L_0$ $\Delta a = a_1 - a_0$ $\Delta b = b_1 - b_0$ $\Delta E_{ab} = \left[\Delta(L)^2 + \Delta(a)^2 + \Delta(b)^2 \right]$	L—lightness A—redness B—yellowness	Schanda [46]

2.4. Characterization of Activated Sodium Bentonite

The structural composition of bentonite was studied by Fourier-transform infrared spectroscopy (FTIR) spectra, which was obtained by mixing 2 mg of Na-Mt powder with 200 mg potassium bromide (KBr). The powder was introduced into molds and pressed at 10 ton/cm^{-2} to obtain the transparent pellets, which were analyzed by a Bruker Tensor 27 spectrometer, and the infrared spectra in transmission mode were recorded in the 4000–400 cm^{-1} frequency region. The microstructural characterization of the Na-Mt was performed by scanning electron microscope (FEI QUANTA 400 SEM/ESEM, Fei Quanta, Hillsboro, WA, USA) and the chemical composition of the bentonite was estimated (Table 3) using the energy dispersive X-ray spectroscopy (EDS/EDAX, PAN'alytical X'Pert PRO, Davis, CA, USA).

Table 3. Chemical composition of activated sodium bentonite (Na-Mt), by EDS/EDAX [38].

Element	Mass Concentration (wt (%))
%Si	69.49
%Al	17.67
%Fe	2.95
%Mg	2.73
%Ca	2.00
%Na	2.76
%K	1.37
%S	1.03

The textural parameters of the bentonite were obtained from N_2 adsorption–desorption isotherms at 77 K using a Micromeritics ASAP 2020 apparatus (TriStar II Plus, Micromeritics Instrument Corporation, Norcross, GA, USA). The bentonite sample was degassed at 150 °C up to 10^{-4} Torr before analysis. The specific surface area (SBET) was then measured by applying Gurevitsch's rule at a relative pressure $p/p_0 = 0.30$ and according to the Brunauer, Emmet, Teller (BET) method from the linear part of the nitrogen adsorption isotherms. Different pore volumes were determined by the Barrett, Joyner, Halenda model (BJH model).

From FTIR analysis (Figure 1) [38], Na-Mt exhibits the stretching vibration of structural O–H groups at 3645 cm^{-1}, structural Si–O groups at 1103, 999 and 789 cm^{-1}, structural Al–O–Al–OH groups at 902 cm^{-1}, structural Al–O–Fe–OH groups at 883 cm^{-1}, the free and interlayer water in bond stretching vibration at 3396 cm^{-1} and adsorbed water yielded bending at 1643 cm^{-1} [47–50].
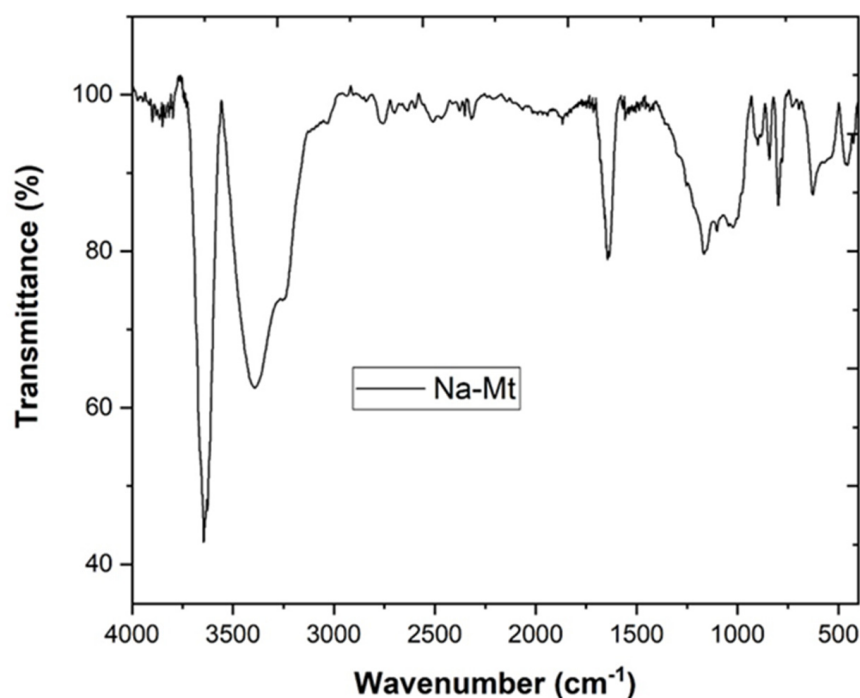

Figure 1. Fourier-transform infrared spectroscopy (FTIR) spectra of Na-Mt.

The results obtained by BET analysis showed that bentonite exhibited a mesoporous structure with a specific surface area of 8.8 m^2/g, a total pore volume of 0.045 cm^3/g and a particle size of 4.0 nm. The respective isotherms can be classified as type II, where unrestricted monolayer–multilayer adsorption occurs, and the behavior of the hysteresis loops can be associated with type H3, which usually corresponds to aggregates of plate-like particles forming slit-like pores [51], which is in agreement with these material structures.

2.5. Adsorption Experimental Setup

The adsorption of organic matter from WW on Na-Mt material was studied in detail (Figure 2), in order to predict the amount of organic carbon that was removed through adsorption. The adsorption process was optimized as follows:

1. Variation of pH (2.0–11) under the following operational conditions: [Na-Mt] = 3.0 g/L, V = 500 mL, agitation 350 rpm, T = 298 K, t = 24 h;
2. Variation of Na-Mt dosage (0.5–10 g/L) under the following operational conditions: pH = 3.0, V = 500 mL, agitation 350 rpm, T = 298 K, t = 24 h.
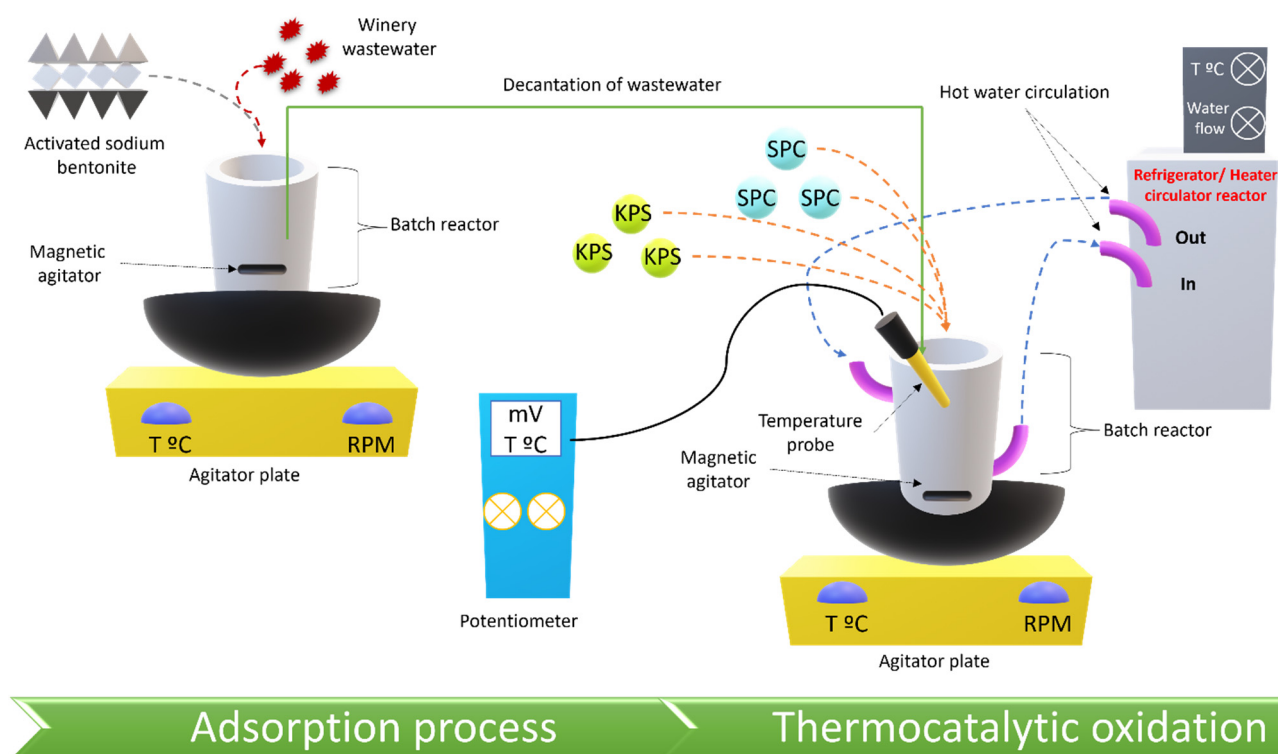   After 24 h, samples were centrifuged and filtrated for analysis.

Figure 2. Illustration of the adsorption and thermocatalytic oxidation processes.

2.6. Thermocatalytic Experimental Setup

The thermocatalytic oxidation process (Figure 2) was carried out by a refrigerator/heater circulator reactor (Julabo F25, Seelbach, Germany). The heater is equipped with a power of 2.2 kW and the refrigerator as a power of 0.170 kW. To achieve the maximum removal efficiency, thermocatalytic experiments were carried as follows:

1. Variation of $S_2O_8^{2-}/H_2O_2$ ratio (1:0; 1:0.25; 1:0.50; 1:0.75; 1:1; 1:1.5) under the following operational conditions: $[S_2O_8^{2-}]$ = 1.0 g/L, pH = 11.0, T = 333 K, agitation 350 rpm, t = 2 h;
2. Variation of $S_2O_8^{2-}/H_2O_2$ dosage (0.1:0.025; 0.5:0.125; 1:0.25; 1.5:0.375; 2:0.5) under the following operational conditions: $S_2O_8^{2-}/H_2O_2$ ratio = 1:0.25, pH = 11.0, T = 333 K, agitation 350 rpm, t = 2 h;
3. Variation of pH (3.0, 5.0, 7.0, 9.0, 11) under the following operational conditions: $S_2O_8^{2-}/H_2O_2$ ratio = 1:0.25, $S_2O_8^{2-}/H_2O_2$ dosage = 0.1:0.025 (*g/g*), T = 333 K, agitation 350 rpm, t = 2 h;
4. Variation of temperature (303, 313, 323, 333 and 343 K) under the following operational conditions: $S_2O_8^{2-}/H_2O_2$ ratio = 1:0.25, $S_2O_8^{2-}/H_2O_2$ dosage = 0.1:0.025 (*g/g*), pH = 7.0, agitation 350 rpm, t = 2 h.

After 2 h, samples were centrifuged and filtrated for analysis. The percentage of contaminant removed through adsorption and thermocatalytic oxidation was calculated in accordance to Equation (2) [52], as follows:

$$X_i = \frac{C_0 - C_f}{C_0} \times 100 \tag{2}$$

where (X_i) of water contamination represents turbidity, TSS, COD and total polyphenol; C_0 and C_f are the initial and final concentrations, respectively.

2.7. Statistical Analysis

All experiments were performed at least in duplicate and the observed standard deviation was always less than 5% of the reported value. Statistical analysis was performed using one-way analysis of variance (ANOVA) and differences were considered significant when $p < 0.05$. Average values were compared using Tukey's test. The statistical analyses were performed using OriginLab 2019 software (Northampton, MA, USA). The data are presented as mean and standard error (mean $\pm$ SE).

3. Results and Discussion

3.1. Adsorption Experiments with Bentonite

3.1.1. Effect of pH

The ability of activated sodium Bentonite (Na-Mt) to adsorb and remove the organic content from the WW was accessed at different pH conditions (2.0–11.0), under the following operational conditions: [Na-Mt] = 3.0 g/L, V = 500 mL, agitation 350 rpm, T = 298 K, t = 24 h. It is known that the variable charge of montmorillonite is significantly affected by pH, due to the ionization of its external hydroxyl groups [53]. At pH lower than pH_{pzc} (pH at the point of zero charge), the clay exhibits anionic exchange capacity, while at pH greater than pH_{pzc}, the clay displays high cation-exchange capacity. In the case of bentonite, it renders negative charge on its surface due to its isomorphous substitution of Al^{3+} for Si^{4+} in tetrahedral layer and Mg^{2+} for Al^{3+} in octahedral sheet and therefore can attract positively charged pollutants [14,54]. However, as observed by several authors [55,56], the mechanism of adsorption on clays is mainly controlled by the adsorption on its interlayer region, since about 85–90% of the available sites for adsorption are located on its internal surface. In this way, the permanent negative charge of montmorillonite is compensated by the cation exchange process, where the initial Na^+ ions may be replaced by positively charged species. Therefore, the contaminant uptake will significantly depend on its charge at given pH [53].

The results in Figure 3, showed a significant increase in TOC removal from pH 2.0 to 3.0 (48.0 and 54.9%, respectively), decreasing as the pH increased to 5.0, 7.0, 9.0 and 11.0 (52.2, 50.2, 49.9 and 41.2%, respectively). In this work, the higher adsorption capacity obtained at pH 3.0, was probably related with the concentration of amphoteric flavylium species present in the WW, making them potentially treated by adsorption. Thus, at pH 3.0 these species acquired positive charge and exchanged the Na^+ ions initially adsorbed on the interlayer region [53]. Increasing the pH > 3.0, the isoelectric point of bentonite was reached (pH = 7) [57], decreasing the bentonite adsorption capacity. In a study performed by Sharma et al. [58] it was observed that the adsorption capacity of methyl blue, anionic dye, onto the clay was decreased with the increase in initial pH of the suspension to alkaline pH. Therefore, considering these results, pH 3.0 was selected as the best pH for the adsorption process.

3.1.2. Effect of Na-Mt Dosage

In the previous section, it was observed that the pH had a significant effect in the adsorption process of WW by Na-Mt. However, the effect of Na-Mt dosage in adsorption process is still unknown; therefore, in this section it was varied the Na-Mt dosage (0.5–10.0 g/L) under the following operational conditions: pH = 3.0, V = 500 mL, agitation 350 rpm, T = 298 K, t = 24 h.

In Figure 4, it was observed an increase in TOC removal, with the increase in Na-Mt dosage from 0.5 to 5.0 g/L (39.5 to 61.1%, respectively). From 5.0 to 10.0 g/L Na-Mt, a small decrease in TOC removal was observed from 61.1 to 56.3%, respectively. Therefore, the application of Na-Mt dosages higher than 5.0 g/L were not considered viable, due to the low TOC removal results, as well as from an economic point of view, due to high Na-Mt application. In the work of Guimarães et al. [53] and Jorge et al. [11] it was also observed that application of clay concentrations higher than 3.0 g/L were not suitable for adsorption process of organic matter of WW.
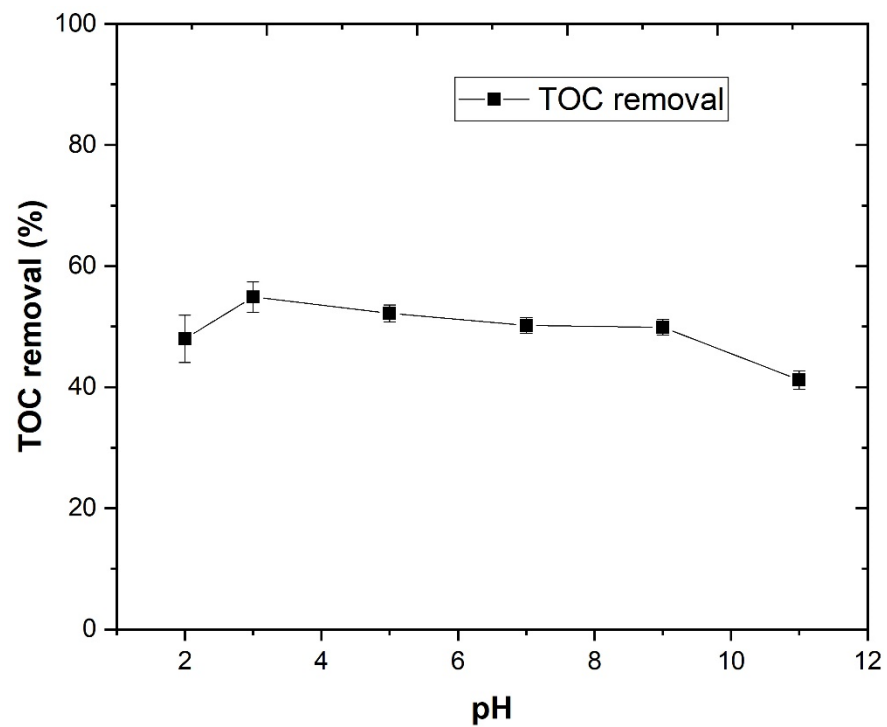
Figure 3. Effect of pH (2.0–11.0) in WW organic matter adsorption onto Na-Mt, under the following operational conditions: [Na-Mt] = 3.0 g/L, V = 500 mL, agitation 350 rpm, T = 298 K, t = 24 h.
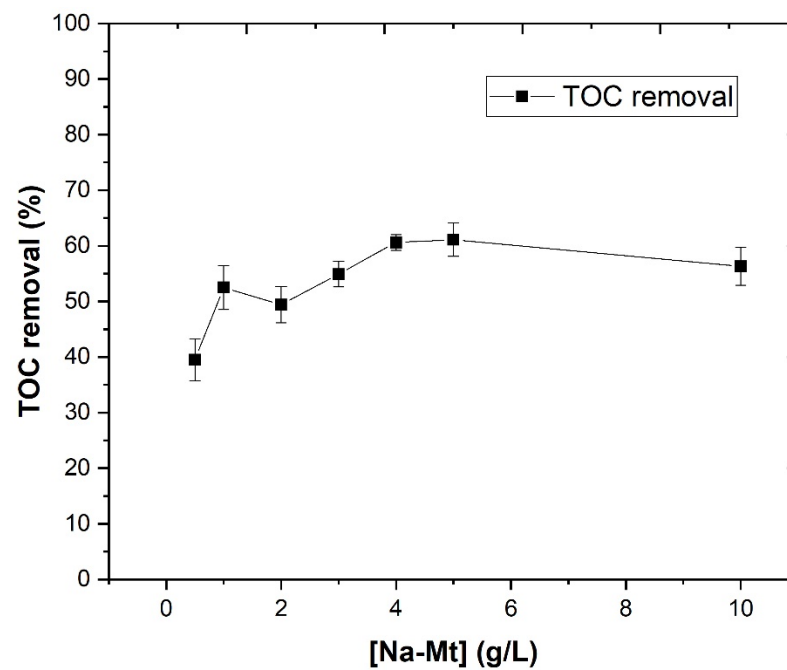

Figure 4. Effect of Na-Mt dosage variation (0.5–10.0 g/L) in adsorption of organic matter from WW onto Na-Mt, under the following operational conditions: pH = 3.0, V = 500 mL, agitation 350 rpm, T = 298 K, t = 24 h.

Therefore, based on these results, the Na-Mt dosage of 5.0 g/L was selected as the most efficient dosage for the adsorption process.

3.2. Thermocatalytic Oxidation with KPS and SPC

3.2.1. SPC Releasing Mechanism

In the previous section, it was observed that the adsorption process was efficient for the removal of organic matter from WW. However, in order to achieve more substantial values an additional process is required. Therefore, a thermocatalytic oxidation process was performed in this work, in which potassium persulfate (KPS) was used in combination with sodium percarbonate (SPC) as oxidant agents. To decrease the use of iron, high temperatures were used for the activation of the oxidants. However, in order to perform this treatment, it was first necessary to understand the dissociation of SPC in water as observed in Equations (3) and (4) [59]. Table 4 shows an assay, in which SPC was applied under different concentrations (0.1–1.0 g/L) in water. The results showed that the theoretical H_2O_2 concentration was very similar to the measured H_2O_2 concentration, by titanium (IV) oxysulfate. TOC results showed a significant decrease from 1.226 to 1.039 to 0.0 mg C/L, respectively, for 0.1, 0.5 and 1.0 g/L of SPC. These results were in agreement to Cui et al. [32], who observed the decomposition of SPC into CO_2, water and small amounts of sodium carbonate.
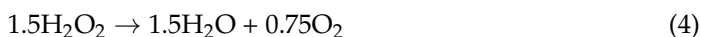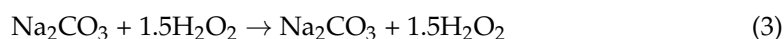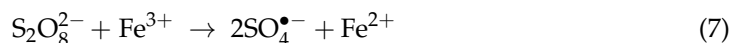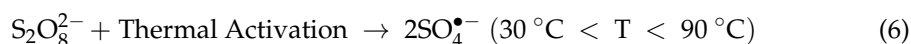
$$Na_2CO_3 + 1.5H_2O_2 \rightarrow Na_2CO_3 + 1.5H_2O_2 \tag{3}$$

$$1.5H_2O_2 \rightarrow 1.5H_2O + 0.75O_2 \tag{4}$$

Table 4. Sodium percarbonate release mechanism.

[SPC]	[H_2O_2] Theoretical	[H_2O_2] Measured	TOC
g/L	mg/L	mg/L	mg C/L
0.1	32.5	22.7	0.000
0.5	162.4	140.3	0.000
1.0	324.8	354.5	0.000

3.2.2. Effect of $S_2O_8^{2-}/H_2O_2$ Ratio

In the works of Rodríguez-Chueca et al. [60,61], the WW was treated by SR-AOPs, in which sulfate radicals were activated by metallic catalysts, UV radiation and heat. Although persulfate reagent can act alone as an oxidant, its effectiveness is limited for oxidation of WW [62]. The generation of sulfate radicals during the persulfate oxidation process can be significantly investigated using different applications, such as UV radiation, heat and iron ions, as observed in Equations (5)–(7) [63], as follows:

$$S_2O_8^{2-} + hv \rightarrow 2SO_4^{\bullet-} \tag{5}$$

$$S_2O_8^{2-} + \text{Thermal Activation} \rightarrow 2SO_4^{\bullet-} \ (30\,^\circ C < T < 90\,^\circ C) \tag{6}$$

$$S_2O_8^{2-} + Fe^{3+} \rightarrow 2SO_4^{\bullet-} + Fe^{2+} \tag{7}$$

The $SO_4^{\bullet-}$ may initiate the production of other intermediate highly reactive oxygen species (ROS), such as hydroxyl radicals ($HO^\bullet$), as observed in Equation (8) [64], as follows:

$$SO_4^{\bullet-} + H_2O \rightarrow HSO_4^- + HO^\bullet \tag{8}$$

However, the use of metallic catalysts for the activation of sulfate radicals have the disadvantage of leaching, becoming toxic for the environment [65]; therefore, this work tested the activation of persulfate radicals by heat without addition of metallic catalyst. In addition, H_2O_2 reagent was used to activate persulfate and initiate sulfate radicals during the oxidation of the WW. To evaluate the performance of H_2O_2 in enhancing persulfate oxidation, the ratio $S_2O_8^{2-}/H_2O_2$ (1:0; 1:0.25; 1:0.50; 1:0.75; 1:1; 1:1.5) was initially studied

under the following operational conditions: $[S_2O_8^{2-}]$ = 1.0 g/L, pH = 11.0, T = 333 K, agitation 350 rpm, t = 2 h.

In observation of Figure 5, without oxidant addition, thermal oxidation achieved 20.6% TOC removal after 2 h of reaction, possibly, due to the evaporation of alcohol or the degradation of some phenolic compounds present in the WW. However, the WW has recalcitrant compounds in its composition, which were not degraded by heat. With application of the oxidant agents, it was observed a TOC removal of 62.6, 63.4, 61.3, 63.3, 54.0 and 55.1%, respectively. The highest TOC removal was observed with application of $S_2O_8^{2-}$/H_2O_2 ratio of 1:0.25 (g/g). With the increase in this ratio, the sulfate radicals initiated scavenging reactions for $HO^\bullet$ radicals, thus decreasing the reactions efficiency, as observed by Equation (9) [62,66], as follows:
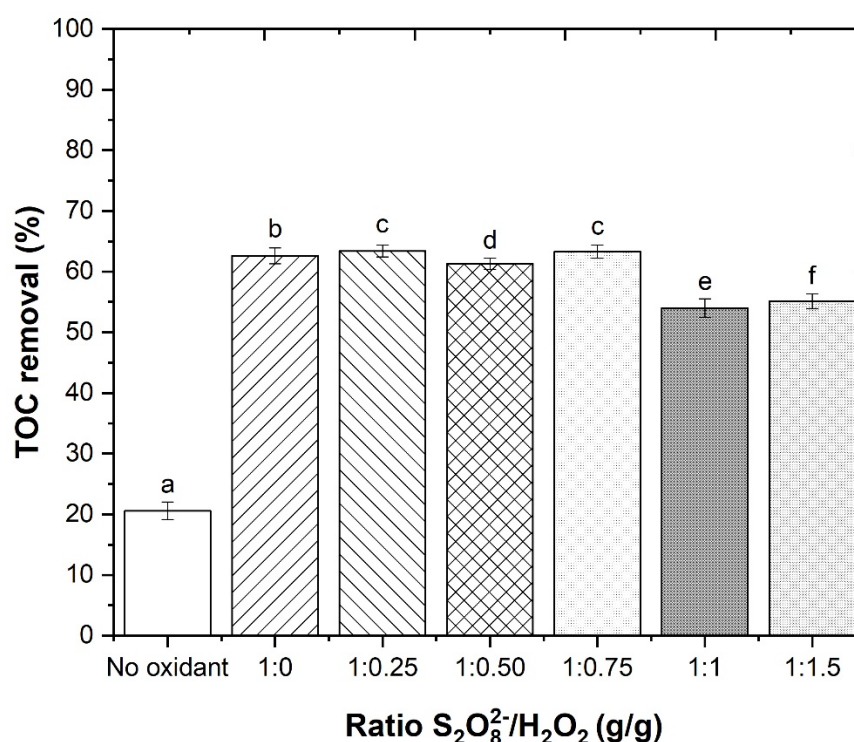
$$SO_4^{2-} + HO^\bullet \rightarrow SO_4^{\bullet-} + HO^- \tag{9}$$

Figure 5. Evolution of TOC removal throughout different $S_2O_8^{2-}$/H_2O_2 ratio (1:0–1:1.5) in thermocatalytic oxidation, under the following operational conditions: $[S_2O_8^{2-}]$ = 1.0 g/L, pH = 11.0, T = 333 K, agitation 350 rpm, t = 2 h. A blank experiment under the following operational conditions is also shown as reference: pH = 11.0, T = 333 K, agitation 350 rpm, t = 2 h. Means in bars with different letters represent significant differences ($p < 0.05$) between each ratio.

Therefore, based in these results, the ratio 1:0.25 (g/g) $S_2O_8^{2-}$/H_2O_2 was selected as the best ratio.

3.2.3. Effect of $S_2O_8^{2-}$/H_2O_2 Dosage

In the previous section it was observed that the ratio of $S_2O_8^{2-}$/H_2O_2 had a high influence in the TOC removal of WW. In this section the dosage of $S_2O_8^{2-}$/H_2O_2 was varied (0.1:0.025; 0.5:0.125; 1:0.25; 1.5:0.375; 2:0.5) under the following operational conditions: $S_2O_8^{2-}$/H_2O_2 ratio = 1:0.25, pH = 11.0, T = 333 K, agitation 350 rpm, t = 2 h. By observation of Figure 6, there was a TOC removal of 63.4, 59.2, 63.4, 56.4 and 59.0%, respectively, for 0.1:0.025; 0.5:0.125; 1:0.25; 1.5:0.375; 2:0.5. These results showed that by decreasing the oxidant concentrations from 1:0.25 to 0.1:0.025 g/g, the TOC removal was similar. However,

by increasing $S_2O_8^{2-}$/H_2O_2 dosage to 2:0.5 g/g, the TOC removal had a higher decrease. These results were different than those observed in the work of Hilles et al. [63], who required an increase in $S_2O_8^{2-}$/H_2O_2 dosage to achieve higher COD removal for landfill leachate treatment. One explanation for these results could be the reduction of scavenging reactions by sulfate and hydroxyl radicals, as previously observed Hilles et al. [66].
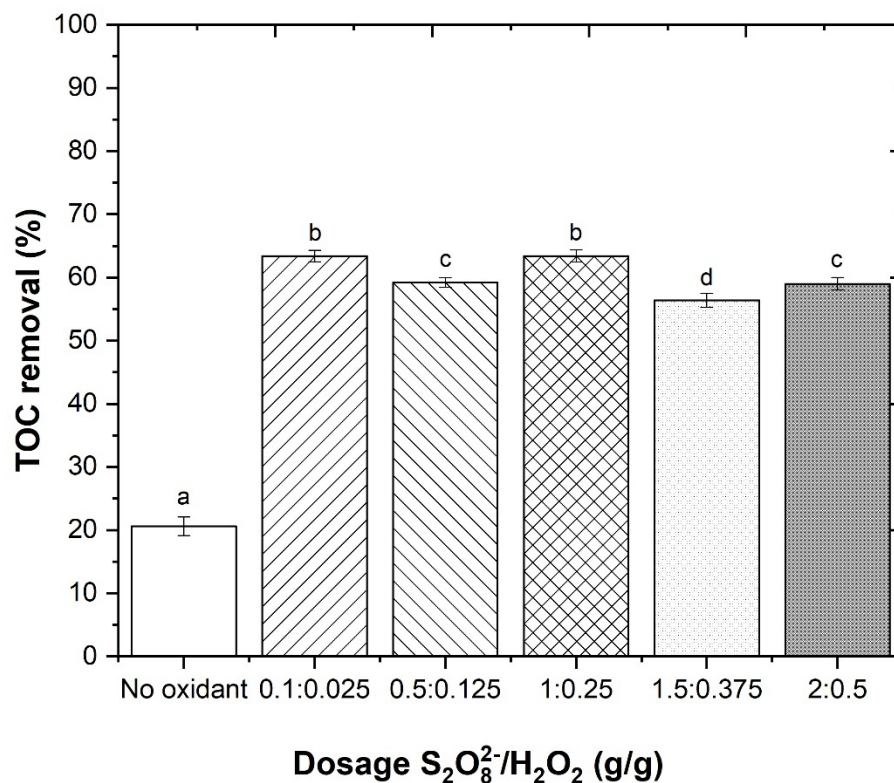

Figure 6. Evolution of TOC removal throughout different $S_2O_8^{2-}$/H_2O_2 dosage (0.1:0.025–2:0.5 g/g) in thermocatalytic oxidation, under the following operational conditions: $S_2O_8^{2-}$/H_2O_2 ratio = 1:0.25, pH = 11.0, T = 333 K, agitation 350 rpm, t = 2 h. A blank experiment under the following operational conditions is also shown as reference: pH = 11.0, T = 333 K, agitation 350 rpm, t = 2 h. Means in bars with different letters represent significant differences ($p < 0.05$) between each dosage.

Therefore, based in these results, $S_2O_8^{2-}$/H_2O_2 dosage 0.1:0.025 g/g was selected as the best dosage.

3.2.4. Effect of pH

After the determination of the best dosage of $S_2O_8^{2-}$/H_2O_2 for thermocatalytic oxidation treatment of WW, it was necessary to optimize the pH of the reaction. In the work of Candia-Onfray et al. [67], the SR-AOPs were performed at pH 5.6. However, in the work of Rodríguez-Chueca et al. [61], the SR-AOPs were performed at pH 6.5 for the treatment of winery wastewater. Due to the large pH spectrum of SR-AOP action, in this section different pH values (3.0, 5.0, 7.0, 9.0, 11.0) were tested under the following operational conditions: $S_2O_8^{2-}$/H_2O_2 ratio = 1:0.25, $S_2O_8^{2-}$/H_2O_2 dosage = 0.1:0.025 (g/g), T = 333 K, agitation 350 rpm, t = 2 h. Figure 7, shows a TOC removal of 59.4, 60.7, 60.4, 52.8 and 63.4%, respectively, after 2 h of reaction, for pH 3.0, 5.0, 7.0, 9.0 and 11.0. With the increase in pH from 3.0 to 11.0 an increase in TOC removal was observed, which was expected, because in the work of Hilles et al. [63], the increase in pH in the $S_2O_8^{2-}$/H_2O_2 system lead to higher COD removal in the treatment of landfill leachate. At high pH conditions (pH 11.0), the alkaline activation was very productive in generating sulfate ions and hydroxyl radicals, which have high oxidation potential ($E_{HO\bullet}^o$ = 2.80 V and $E_{SO_4^-}^o$ = 2.70 V) [19].

Furman et al. [68] also observed that persulfate's efficiency in oxidation processes increased in alkaline conditions. For base activation of persulfate, a nucleophilic attack on the O–O bond is considered as the main mechanism as observed in Equations (10) and (11) [19]. The perhydroxyl radicals ($HO_2^\bullet$) plays a key role in the production of sulfate radicals. At acidic pH, the superoxide radicals tend to react with hydrogen ions to form perhydroxyl radicals, while at alkaline pH, perhydroxyl radicals tends to decompose into superoxide radicals. Due to alkaline conditions, the sulfate radicals are transformed into hydroxyl radicals as observed in Equation (12) [69], as follows:
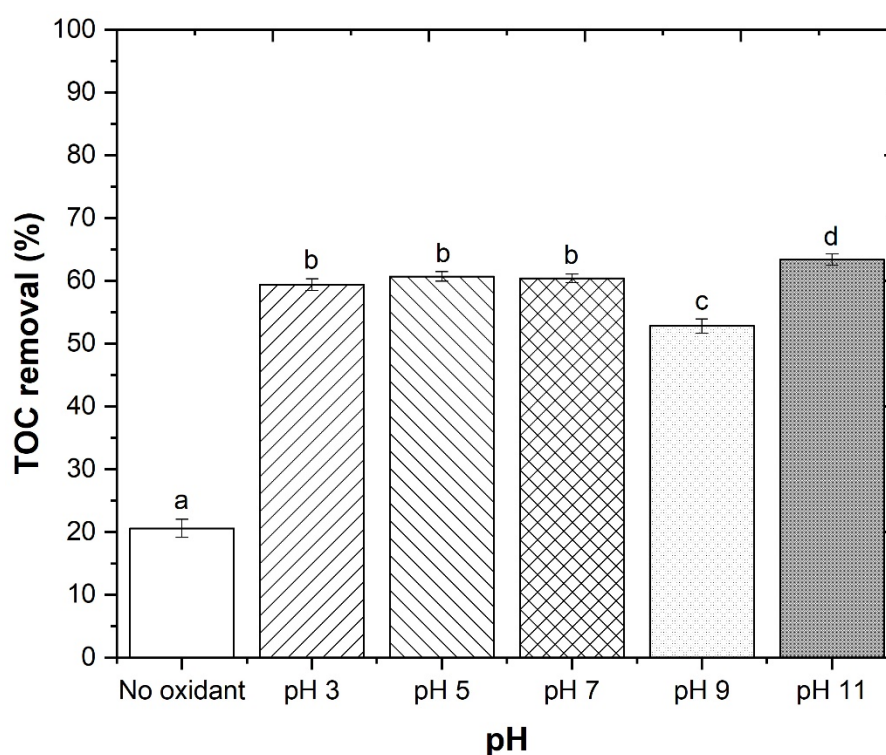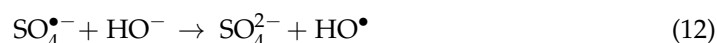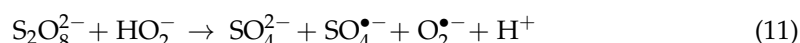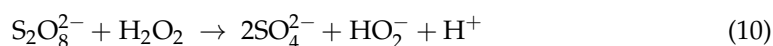
$$S_2O_8^{2-} + H_2O_2 \rightarrow 2SO_4^{2-} + HO_2^- + H^+ \tag{10}$$

$$S_2O_8^{2-} + HO_2^- \rightarrow SO_4^{2-} + SO_4^{\bullet-} + O_2^{\bullet-} + H^+ \tag{11}$$

$$SO_4^{\bullet-} + HO^- \rightarrow SO_4^{2-} + HO^\bullet \tag{12}$$

Figure 7. Evolution of TOC removal at different pH (3.0–11.0) in thermocatalytic oxidation, under the following operational conditions: $S_2O_8^{2-}$/H_2O_2 ratio = 1:0.25, $S_2O_8^{2-}$/H_2O_2 dosage = 0.1:0.025 (g/g), T = 333 K, agitation 350 rpm, t = 2 h. A blank experiment under the following operational conditions is also shown as reference: pH = 11.0, T = 333 K, agitation 350 rpm, t = 2 h. Means in bars with different letters represent significant differences ($p < 0.05$) between each pH.

Despite the high TOC removal at pH 11.0, there were several associated disadvantages, such as (1) the high cost in reagents to achieve pH 11.0 and (2) the Portuguese law No. 236/98 for residual water discharge for the pH of the treated wastewater is 6.0 to 9.0. Considering the similar TOC removal between pH 7.0 (60.4%) and pH 11 (63.4%), pH 7.0 was selected as the best pH.

3.2.5. Effect of Temperature

The bond energy of O–O of persulfate is estimated to be in the range of 140–213.3 kJ/mol. The essential mechanism of persulfate activation is the fission of O–O bond in the structure of persulfate. For heat activation, the energy input by the high temperature (>50 °C) can cause the fission of O–O bond to form the sulfate radicals, as observed by Equation (7) [19]. The

hydroxyl radicals are the main radicals produced during the heat activation of persulfate, indicating that sulfate radicals are quickly transformed into hydroxyl radicals, as observed in Equation (13) [70], as follows:

$$SO_4^{\bullet -} + H_2O \rightarrow SO_4^{2-} + HO^{\bullet} + H^+ \tag{13}$$
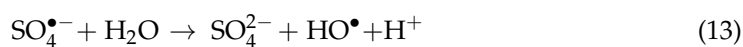
Therefore, in this section the effect of temperature variation (303, 313, 323, 333 and 343 K) was studied under the following operational conditions: $S_2O_8^{2-}/H_2O_2$ ratio = 1:0.25, $S_2O_8^{2-}/H_2O_2$ dosage = 0.1:0.025 (g/g), pH = 7.0, agitation 350 rpm, t = 2 h. Initial blank experiments were performed without addition of oxidant (Figure 8) and a TOC removal of 39.7, 48.0, 59.2, 20.6 and 63.4%, respectively, was observed. With the increase in temperature, an increase in TOC removal was observed, which indicated that there were organic compounds susceptible to heat. When oxidant agents ($S_2O_8^{2-}/H_2O_2$) were added, an increase in TOC removal to 52.9, 53.0, 60.2, 60.4 and 65.6%, respectively, was observed. These results were similar to the work of Rodríguez-Chueca et al. [61], who observed that when increasing the temperature, the efficiency of oxidation reaction of sulfate radicals increased in COD removal of WW. In the work of Zrinyi and Pham [71], it was observed that phenol degradation by sulfate radicals was more efficient at 343 K, which is in agreement with this work.
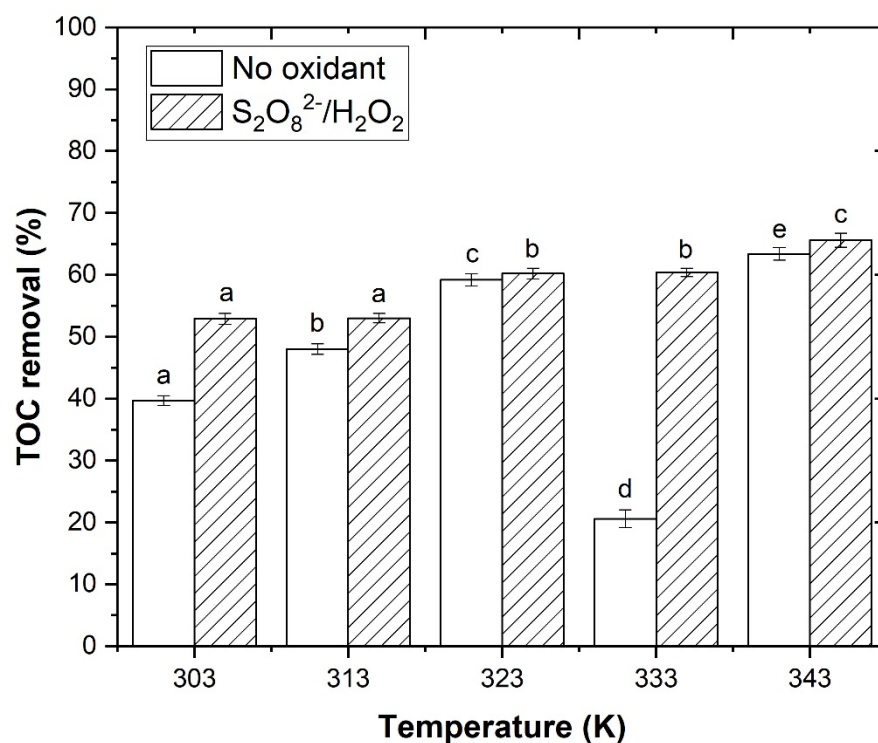

Figure 8. Evolution of TOC removal at different temperatures (303–343 K) in thermocatalytic oxidation, under the following operational conditions: $S_2O_8^{2-}/H_2O_2$ ratio = 1:0.25, $S_2O_8^{2-}/H_2O_2$ dosage = 0.1:0.025 (g/g), pH = 7.0, agitation 350 rpm, t = 2 h. Blank experiments at different temperatures (303–343 K) are also shown as reference, under the following operational conditions: pH = 7.0, agitation 350 rpm, t = 2 h. Means in bars with different letters represent significant differences ($p < 0.05$) between each process (Blank and thermocatalytic oxidation) by comparing temperatures.

Therefore, based in these results, 343 K was selected as the best temperature for sulfate radical activation.

3.3. Combination of Adsorption with Thermocatalytic Oxidation

In previous sections, it was observed that application of Na-Mt in the adsorption process had high efficiency in the removal of organic carbon from WW. This work also

tested the application of a thermocatalytic process, in which high temperatures and H_2O_2 in the form of SPC were used to activate persulfate radicals, to degrade organic carbon from the WW. The results also showed a high efficiency from this treatment; however, there were some limitations such as high levels of turbidity, TSS and total polyphenols (Table 1), which could have decreased the thermocatalytic oxidation efficiencies. Given the results obtained individually, it will be interesting to study the combination of the two previous processes. In this context, the combination of adsorption process with bentonite was tested in the optimal conditions obtained previously, as follows: [Na-Mt] = 5.0 g/L, pH = 3.0, V = 500 mL, agitation 350 rpm, T = 298 K, t = 24 h, with thermocatalytic oxidation best conditions, as follows: $S_2O_8^{2-}$/H_2O_2 ratio = 1:0.25, $S_2O_8^{2-}$/H_2O_2 dosage = 0.1:0.025 (*g/g*), pH = 7.0, T = 343 K, agitation 350 rpm, t = 2 h). In observation of Figure 9a, the adsorption process had a TOC, COD and a BOD_5 removal of 61.1, 68.4 and 40.7%, respectively. With application of thermocatalytic process, the removals increased to 76.7, 81.4 and 81.7%, respectively. Clearly, the combination of adsorption and thermocatalytic oxidation achieved higher removals than both processes alone. One possible reason for the increased efficiency could be the reduction of interferents present in the WW, such as the turbidity, TSS and total polyphenols. In Figure 9b, turbidity, TSS and total polyphenols reduction of 81.4, 94.3 and 99.4% were observed, respectively. After the thermocatalytic oxidation the removals increased to 92.6, 98.1 and 99.9%, respectively. These results were in agreement with the work of Jaafarzadeh et al. [72], who observed an increase in sulfate radicals efficiency in COD removal of pulp and paper wastewater after reduction of TSS and color reduction. In accordance with Amor et al. [73], the high turbidity, TSS and total polyphenols are considered to be hydroxyl radical scavengers.
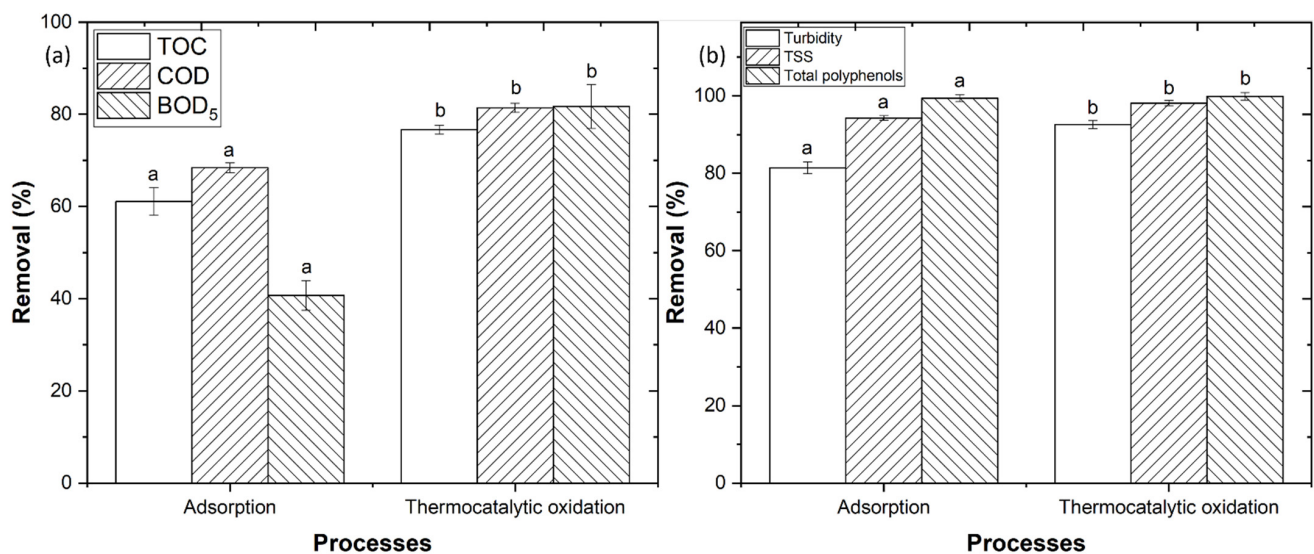

Figure 9. Overall results after adsorption process and thermocatalytic oxidation processes in (**a**) TOC, COD and BOD_5 removal and (**b**) turbidity, TSS and total polyphenols. Adsorption operational conditions, as follows: [Na-Mt] = 5.0 g/L, pH = 3.0, V = 500 mL, agitation 350 rpm, T = 298 K, t = 24 h. Thermocatalytic oxidation conditions, as follows: $S_2O_8^{2-}$/H_2O_2 ratio = 1:0.25, $S_2O_8^{2-}$/H_2O_2 dosage = 0.1:0.025 (*g/g*), pH = 7.0, T = 343 K, agitation 350 rpm, t = 2 h. Means in bars with different letters represent significant differences ($p < 0.05$) between each parameter (TOC, COD, BOD_5, turbidity, TSS and total polyphenols) by comparing wastewaters.

3.4. Phytotoxicity Tests

It was observed that the combination of adsorption process with Na-Mt and thermo-catalytic oxidation with $S_2O_8^{2-}$/H_2O_2 was beneficial for the reduction of organic carbon present in the WW. However, its effect in the germination of plants is still unknown. Therefore, the phytotoxic effect of raw WW, adsorption and combined adsorption–thermocatalytic

oxidation on germination of seeds from two Dicotyledonae (lettuce and cucumber) and two Monocotyledonae (corn and onion) were evaluated, similar to the works of Casa et al. [74] and Mosse et al. [75]. For the determination of the germination index, the seed germination and root elongation (Equation (1)) were considered, which explains results above 100%.

In Figure 10, it was observed that raw WW posed a phytotoxicity effect to onion and lettuce seeds (GI = 58 and 0%), regarding cucumber and corn seeds (106 and 178%, respectively). With application of combined adsorption–thermocatalytic oxidation, an increase in the GI to 176, 134, 250 and 269 %, respectively, was observed for onion, cucumber, lettuce and corn seeds (GI > 80%), which showed that these treatments had a low phytotoxic effect for germination of plants. In the work of Rizzo et al. [76], it was observed that application of an adsorption process for the removal of contaminants increased the germination index of plant seeds, thus decreasing the phytotoxicity of the wastewater, similar to the results obtained in this work. These results evidence the suitability of the combination of adsorption and thermocatalytic oxidation for the reduction of phytotoxicity in seed germination.
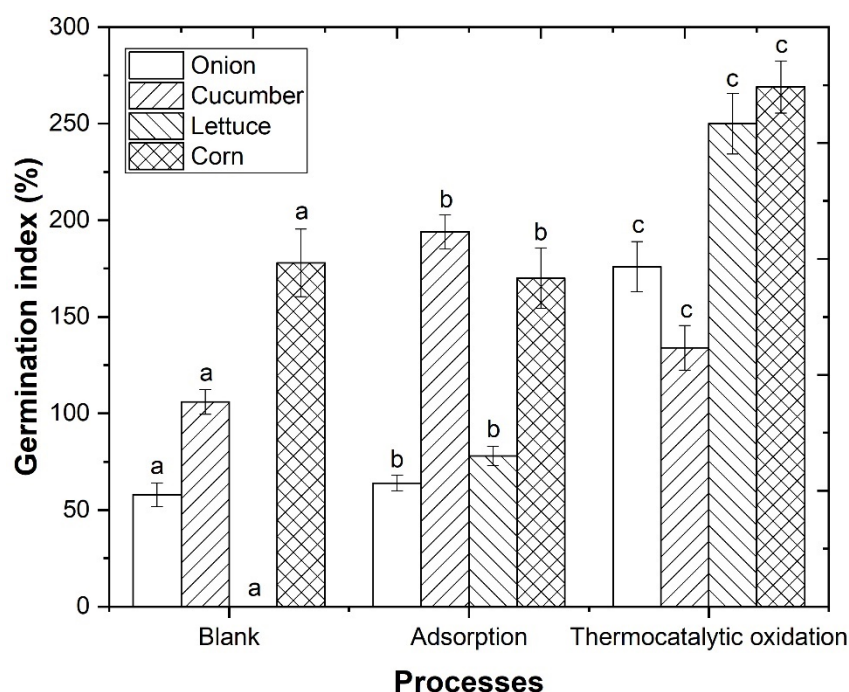

Figure 10. Analysis of seed phytotoxicity after wastewater treatment, by evaluation of germination index (GI). Adsorption operational conditions, as follows: [Na-Mt] = 5.0 g/L, pH = 3.0, V = 500 mL, agitation 350 rpm, T = 298 K, t = 24 h. Thermocatalytic oxidation conditions, as follows: $S_2O_8^{2-}$/H_2O_2 ratio = 1:0.25, $S_2O_8^{2-}$/H_2O_2 dosage = 0.1:0.025 (g/g), pH = 7.0, T = 343 K, agitation 350 rpm, t = 2 h. GI $\leq$ 50% (high concentration of phytotoxic substances), 80% < GI > 50% (moderated presence of phytotoxic substances), GI $\geq$ 80% (there are no phytotoxic substances, or they exist in very small dosages). Means in bars with different letters represent significant differences ($p < 0.05$) between each process (blank, adsorption and thermocatalytic oxidation) by comparing different plant seeds.

As previously observed by Santos et al. [77], polyphenols are responsible for the toxicity of the WW, and their removal by both treatments could have potentiated the increase in the germination index; therefore, the phenolic content of the WW was evaluated (Figure 11), as well as the efficiency of both treatments in its removal. In Figure 11, a high content of total phenols, non-flavonoids and flavonoids (192, 112 and 80 mg gallic acid/L, respectively) was observed, which is in agreement to the work of Li and Sun [78], who observed the presence of these compounds in grapes and red wine.
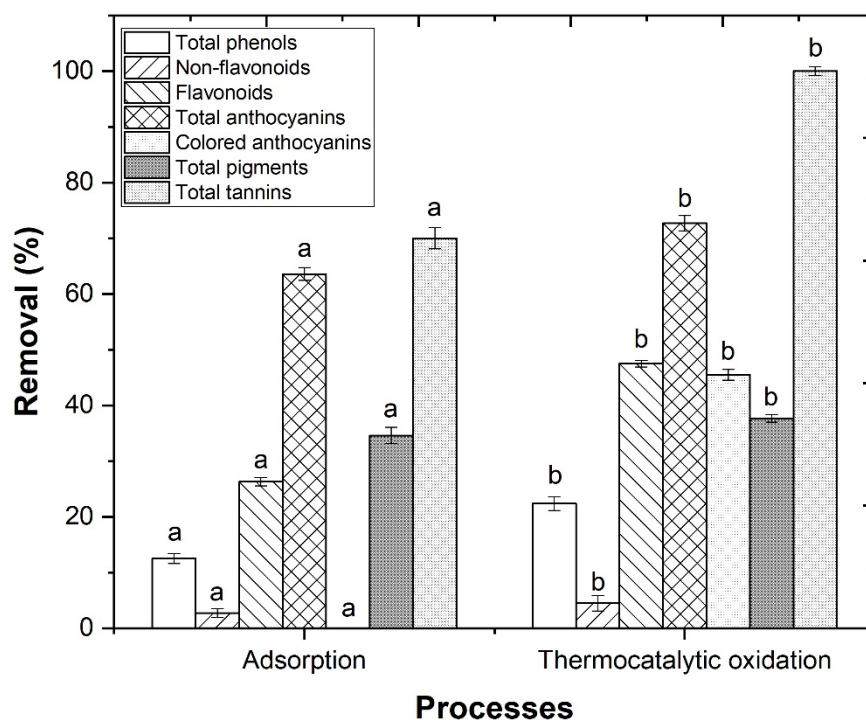
Figure 11. Analysis of phenolic composition after adsorption process and combined adsorption-thermocatalytic oxidation processes. Adsorption operational conditions, as follows: [Na-Mt] = 5.0 g/L, pH = 3.0, V = 500 mL, agitation 350 rpm, T = 298 K, t = 24 h. Thermocatalytic oxidation conditions, as follows: $S_2O_8^{2-}$/H_2O_2 ratio = 1:0.25, $S_2O_8^{2-}$/H_2O_2 dosage = 0.1:0.025 (g/g), pH = 7.0, T = 343 K, agitation 350 rpm, t = 2 h. Means in bars with different letters represent significant differences ($p < 0.05$) between each parameter (total phenols, non-flavonoids, flavonoids, total anthocyanins, colored anthocyanins, total pigments and total tannins) by comparing wastewaters.

In Figure 11, the presence of total anthocyanins (11 mg/L) was observed, which was responsible for the red color of the WW [42]. In accordance with Cheynier et al. [79] the red color is not only derived from anthocyanins, but also from the conversion of grape anthocyanins into other pigments in a process called copigmentation. This was also in agreement with the data from this work, since a certain amount of polymeric and total pigments was also detected (0.81 and 1.62 mg/L respectively).

Another factor which could have an influence on the red color of the WW was the presence of tannins in a large concentration (97 mg/L) which formed tannin–anthocyanin adducts with intense red color [79].

Considering that there are no studies regarding the effect of adsorption and combined adsorption–thermocatalytic oxidation processes in the removal of phenolic compounds of WW, it was evaluated the removal of total phenols, non-flavonoids, flavonoids, total anthocyanins, colored anthocyanins, total pigments and total tannins.

In Figure 11, a removal of 12.5, 2.7, 26.3, 63.6, 0.0, 34.6 and 70.0%, respectively, by adsorption process was observed. With application of combined adsorption–thermocatalytic oxidation process, it was observed a removal of 22.4, 4.5, 47.5, 72.7, 45.5, 37.7 and 100%, respectively. The reduction of these phenolic compounds had an effect on the removal of color from the WW, which was evaluated by a CIELab analysis (Table 5), similar to the work of Jorge et al. [38].

Table 5. Analysis of chromatic characteristics (CIELab) after adsorption process and combined adsorption–thermocatalytic oxidation processes. Adsorption operational conditions, as follows: [Na-Mt] = 5.0 g/L, pH = 3.0, V = 500 mL, agitation 350 rpm, T = 298 K, t = 24 h. Thermocatalytic oxidation conditions, as follows: $S_2O_8^{2-}$/H_2O_2 ratio = 1:0.25, $S_2O_8^{2-}$/H_2O_2 dosage = 0.1:0.025 (g/g), pH = 7.0, T = 343 K, agitation 350 rpm, t = 2 h. Means in the same column with different letters represent significant differences ($p < 0.05$) within each parameter by comparing the different processes.

Processes	Time	L	a	b	ΔL	Δa	Δb	ΔE_{ab}
	(hours)	(%)						
Blank	0	5.9 ± 1.7 a	3.26 ± 1.3 a	3.60 ± 1.5 a				
Adsorption	24	90.5 ± 0.4 b	0.93 ± 0.5 b	2.86 ± 1.9 b	84.5 ± 0.8 a	−2.33 ± 1.0 a	−0.74 ± 1.2 a	84.58 ± 0.3 a
Thermocatalytic oxidation	26	95.5 ± 0.2 c	1.02 ± 1.4 b	8.34 ± 1.5 c	89.6 ± 0.4 b	−2.24 ± 1.6 b	4.74 ± 3.5 b	89.71 ± 0.9 b

With application of adsorption and combined adsorption–thermocatalytic oxidation processes it were observed negative values for Δa (−2.33 and −2.24, respectively), which indicated a reduction of the red color. An increase in the luminosity of the raw WW from 5.9% to 90.5 and 95.5%, respectively was also observed after adsorption and combined adsorption–thermocatalytic processes, which meant that the phenolic compounds were directly linked to the dark red color of the wastewater. The color removal, given by the Euclidean distance was 84.6 and 89.7 after adsorption and combined adsorption–thermocatalytic oxidation processes, meaning that color removal was perceptible to the human eye in accordance with Spagna et al. [45].

4. Conclusions

In this work, two processes were applied for the treatment of WW: adsorption and thermocatalytic oxidation processes. For the adsorption process activated sodium bentonite (Na-Mt) was used, which showed great swelling properties and a high capacity for COD removal from the WW. For the thermocatalytic oxidation process, the sulfate radicals were activated by high temperatures, without metal catalyst, to avoid the production of metal sludge. In addition, to increase the activation of sulfate radicals, H_2O_2 was applied in solid form, by addition of sodium percarbonate (SPC). Considering the objectives defined for this work, the main conclusions are:

1. The adsorption process in bentonite is a very efficient process for organic carbon reduction. Under the best operational conditions: [Na-Mt] = 5.0 g/L, pH = 3.0, V = 500 mL, agitation 350 rpm, T = 298 K, t = 24 h, there is a TOC removal of 61.1%;
2. The sodium percarbonate (SPC) is able to release H_2O_2 into water and the carbonate is evaporated as CO_2;
3. The sulfate radicals can be activated at high temperatures (T = 343 K). Under the best operational conditions: $S_2O_8^{2-}$/H_2O_2 ratio = 1:0.25, $S_2O_8^{2-}$/H_2O_2 dosage = 0.1:0.025 (g/g), pH = 7.0, T = 343 K, agitation 350 rpm, t = 2 h achieving 65.6% TOC removal;
4. The combination of adsorption–thermocatalytic oxidation processes allows efficient WW treatment with a TOC, COD and BOD_5 removal of 76.7, 81.4 and 81.7%, respectively; It is also concluded that the combination of these two processes poses no phytotoxic effect in the germination of seeds due to high germination index (GI > 80%) observed in germination of onion, cucumber, lettuce and corn seeds;
5. The combination of adsorption–thermocatalytic oxidation processes proved to be very efficient in the removal of phenolic compounds present in the WW and the dark red color of the wastewater due to the negative value of Δa (−2.24) and high luminosity (L = 95.5%).

These results showed that the combination of adsorption with bentonite and thermocatalytic processes are very promising to decrease the large content of organic carbon and phytotoxicity present in the WW.

Institutional Review Board Statement: Not applicable.

Informed Consent Statement: Not applicable.

Data Availability Statement: Not applicable.

Conflicts of Interest: The authors declare no conflict of interest.

References

1.   OIV. *State of the World Vitiviniculture Sector in 2020–2021*; OIV: Paris, France, 2020; pp. 1–19.
2.   Ferreira, R.; Gomes, J.; Martins, R.C.; Costa, R.; Quinta-Ferreira, R.M. Winery Wastewater Treatment by Integrating Fenton's Process with Biofiltration by Corbicula Fluminea. *J. Chem. Technol. Biotechnol.* **2018**, *93*, 333–339. [CrossRef]
3.   Ioannou, L.A.; Fatta-Kassinos, D. Solar Photo-Fenton Oxidation against the Bioresistant Fractions of Winery Wastewater. *J. Environ. Chem. Eng.* **2013**, *1*, 703–712. [CrossRef]
4.   Ioannou, L.A.; Puma, G.L.; Fatta-Kassinos, D. Treatment of Winery Wastewater by Physicochemical, Biological and Advanced Processes: A Review. *J. Hazard. Mater.* **2015**, *286*, 343–368. [CrossRef] [PubMed]
5.   Mosteo, R.; Sarasa, J.; Ormad, M.P.; Ovelleiro, J.L. Sequential Solar Photo-Fenton-Biological System for the Treatment of Winery Wastewaters. *J. Agric. Food Chem.* **2008**, *56*, 7333–7338. [CrossRef] [PubMed]
6.   Chatzilazarou, A.; Katsoyannos, E.; Gortzi, O.; Lalas, S.; Paraskevopoulos, Y.; Dourtoglou, E.; Tsaknis, J. Removal of Polyphenols from Wine Sludge Using Cloud Point Extraction. *J. Air Waste Manag. Assoc.* **2010**, *60*, 454–459. [CrossRef] [PubMed]
7.   Mohana, S.; Acharya, B.K.; Madamwar, D. Distillery Spent Wash: Treatment Technologies and Potential Applications. *J. Hazard. Mater.* **2009**, *163*, 12–25. [CrossRef]
8.   Amaral-Silva, N.; Martins, R.C.; Paiva, C.; Castro-Silva, S.; Quinta-Ferreira, R.M. A New Winery Wastewater Treatment Approach during Vintage Periods Integrating Ferric Coagulation, Fenton Reaction and Activated Sludge. *J. Environ. Chem. Eng.* **2016**, *4*, 2207–2215. [CrossRef]
9.   Spennati, E.; Casazza, A.A.; Converti, A. Winery Wastewater Treatment by Microalgae to Production Purposes. *Energies* **2020**, *13*, 2490. [CrossRef]
10.   Marchão, L.; Fernandes, J.R.; Sampaio, A.; Peres, J.A.; Tavares, P.B.; Lucas, M.S. Microalgae and Immobilized TiO$_2$/UV-A LEDs as a Sustainable Alternative for Winery Wastewater Treatment. *Water Res.* **2021**, *203*, 117464. [CrossRef]
11.   Jorge, N.; Teixeira, A.R.; Lucas, M.S.; Peres, J.A. Combination of adsorption in natural clays and photo-catalytic processes for winery wastewater treatment. In *Advances in Geoethics and Groundwater Management: Theory and Practice for a Sustainable Development*; Abrunhosa, M., Chambel, A., Peppoloni, S., Chaminé, H.I., Eds.; Springer: Cham, Switzerland, 2021; pp. 291–294, ISBN 978-3-030-59320-9.
12.   Amor, C.; Rodríguez-Chueca, J.; Fernandes, J.L.; Domínguez, J.R.; Lucas, M.S.; Peres, J.A. Winery Wastewater Treatment by Sulphate Radical Based-Advanced Oxidation Processes (SR-AOP): Thermally vs UV-Assisted Persulphate Activation. *Process Saf. Environ. Prot.* **2019**, *122*, 94–101. [CrossRef]
13.   Domínguez, C.M.; Quintanilla, A.; Casas, J.A.; Rodriguez, J.J. Treatment of Real Winery Wastewater by Wet Oxidation at Mild Temperature. *Sep. Purif. Technol.* **2014**, *129*, 121–128. [CrossRef]
14.   Alexander, J.A.; Abbas, M.; Zaini, A.; Aliyu, E.U.; Omeiza, A.U.; Asanja, J.; Abbas, M.; Zaini, A. Surface Modification of Low-Cost Bentonite Adsorbents-A Review. *Part. Sci. Technol.* **2019**, *37*, 534–545. [CrossRef]
15.   Vieira, M.G.A.; Neto, A.F.A.; Gimenes, M.L.; Silva, M.G.C. Sorption Kinetics and Equilibrium for the Removal of Nickel Ions from Aqueous Phase on Calcined Bofe Bentonite Clay. *J. Hazard. Mater.* **2010**, *177*, 362–371. [CrossRef] [PubMed]
16.   Salazar, F.N.; Marangon, M.; Labbé, M.; Lira, E.; Rodríguez-Bencomo, J.J.; López, F. Comparative Study of Sodium Bentonite and Sodium-Activated Bentonite Fining during White Wine Fermentation: Its Effect on Protein Content, Protein Stability, Lees Volume, and Volatile Compounds. *Eur. Food Res. Technol.* **2017**, *243*, 2043–2054. [CrossRef]
17.   Hu, P.; Long, M. Cobalt-Catalyzed Sulfate Radical-Based Advanced Oxidation: A Review on Heterogeneous Catalysts and Applications. *Appl. Catal. B Environ.* **2016**, *181*, 103–117. [CrossRef]
18.   Huang, J.; Zhang, H. Mn-Based Catalysts for Sulfate Radical-Based Advanced Oxidation Processes: A Review. *Environ. Int.* **2019**, *133*, 105141. [CrossRef]

19. Wang, J.; Wang, S. Activation of Persulfate (PS) and Peroxymonosulfate (PMS) and Application for the Degradation of Emerging Contaminants. *Chem. Eng. J.* **2018**, *334*, 1502–1517. [CrossRef]

20. Romero, A.; Santos, A.; Vicente, F.; González, C. Diuron Abatement Using Activated Persulphate: Effect of pH, Fe (II) and Oxidant Dosage. *Chem. Eng. J.* **2010**, *162*, 257–265. [CrossRef]

21. Liu, H.; Bruton, T.A.; Li, W.; Van Buren, J.; Prasse, C.; Doyle, F.M.; Sedlak, D.L. Oxidation of Benzene by Persulfate in the Presence of Fe (III)-and Mn (IV)-Containing Oxides: Stoichiometric Efficiency and Transformation Products. *Environ. Sci. Technol.* **2016**, *50*, 890–898. [CrossRef]

22. Bolobajev, J.; Trapido, M.; Goi, A. Improvement in Iron Activation Ability of Alachlor Fenton-like Oxidation by Ascorbic Acid. *Chem. Eng. J.* **2015**, *281*, 566–574. [CrossRef]

23. Govindan, K.; Raja, M.; Noel, M.; James, E.J. Degradation of Pentachlorophenol by Hydroxyl Radicals and Sulfate Radicals Using Electrochemical Activation of Peroxomonosulfate, Peroxodisulfate and Hydrogen Peroxide. *J. Hazard. Mater.* **2014**, *272*, 42–51. [CrossRef] [PubMed]

24. Giannakis, S.; Vives, F.A.G.; Grandjean, D.; Magnet, A.; De Alencastro, L.F.; Pulgarin, C. Effect of Advanced Oxidation Processes on the Micropollutants and the Effluent Organic Matter Contained in Municipal Wastewater Previously Treated by Three Different Secondary Methods. *Water Res.* **2015**, *84*, 295–306. [CrossRef]

25. Monteagudo, J.M.; Durán, A.; Latorre, J.; Expósito, A.J. Application of Activated Persulfate for Removal of Intermediates from Antipyrine Wastewater Degradation Refractory towards Hydroxyl Radical. *J. Hazard. Mater.* **2016**, *306*, 77–86. [CrossRef] [PubMed]

26. Gu, X.; Lu, S.; Li, L.; Qiu, Z.; Sui, Q.; Lin, K.; Luo, Q. Oxidation of 1, 1, 1-Trichloroethane Stimulated by Thermally Activated Persulfate. *Ind. Eng. Chem. Res.* **2011**, *50*, 11029–11036. [CrossRef]

27. Tan, C.; Gao, N.; Zhou, S.; Xiao, Y.; Zhuang, Z. Kinetic Study of Acetaminophen Degradation by UV-Based Advanced Oxidation Processes. *Chem. Eng. J.* **2014**, *253*, 229–236. [CrossRef]

28. Mahdi-ahmed, M.; Chiron, S. Ciprofloxacin Oxidation by UV-C Activated Peroxymonosulfate in Wastewater. *J. Hazard. Mater.* **2014**, *265*, 41–46. [CrossRef]

29. Karthikeyan, S.; Boopathy, R.; Sekaran, G. In Situ Generation of Hydroxyl Radical by Cobalt Oxide Supported Porous Carbon Enhance Removal of Refractory Organics in Tannery Dyeing Wastewater. *J. Colloid Interface Sci.* **2015**, *448*, 163–174. [CrossRef] [PubMed]

30. Ghanbari, F.; Moradi, M.; Gohari, F. Degradation of 2,4,6-Trichlorophenol in Aqueous Solutions Using Peroxymonosulfate/Activated Carbon/UV Process via Sulfate and Hydroxyl Radicals. *J. Water Process Eng.* **2016**, *9*, 22–28. [CrossRef]

31. Devi, P.; Das, U.; Dalai, A.K. In-Situ Chemical Oxidation: Principle and Applications of Peroxide and Persulfate Treatments in Wastewater Systems. *Sci. Total Environ.* **2016**, *571*, 643–657. [CrossRef]

32. Cui, H.; Gu, X.; Lu, S.; Fu, X.; Zhang, X.; Fu, G.Y.; Qiu, Z.; Sui, Q. Degradation of Ethylbenzene in Aqueous Solution by Sodium Percarbonate Activated with EDDS–Fe (III) Complex. *Chem. Eng. J.* **2017**, *309*, 80–88. [CrossRef]

33. APHA; AWWA; WEF. *Standard Methods for the Examination of Water and Wastewater*, 20th ed.; American Public Health Association: Washington, DC, USA; American Water Works Association: Denver, CO, USA; Water Environment Federation: Alexandria, VR, USA, 1999.

34. Singleton, V.L.; Rossi, J.A. Colorimetry of Total Phenolics with Phosphomolybdic-Phosphotungstic Acid Reagents. *Am. J. Enol. Vitic.* **1965**, *16*, 144–158.

35. OECD. *OECD Guidelines for the Testing of Chemicals: Terrestrial Plant Test*; OECD: Paris, France, 2004; Volume 208.

36. Varnero, M.T.; Rojas, C.; Orellana, R. Índices de Fitotoxicidad en Residuos Orgánicos Durante el Compostaje. *Rev. Cienc. Suelo Nutr. Veg.* **2007**, *7*, 28–37. [CrossRef]

37. Tiquia, S.M.; Tam, N.F.Y. Elimination of Phytotoxicity during Co-Composting of Spent Pig-Manure Sawdust Litter and Pig Sludge. *Bioresour. Technol.* **1998**, *65*, 43–49. [CrossRef]

38. OIV. *Compendium of International Methods of Wine and Must Analysis-Volume I*, 2017th ed.; OIV: Paris, France, 2017; ISBN 979-10-91799-64-5.

39. Curvelo-Garcia, A. Controlo de qualidade dos vinhos. In *Química Enológica e Métodos Analíticos. Avanços Recentes no Controlo da Qualidade de Vinhos e de Outros Produtos Vitivinícolas*; Curvelo-Garcia, A.S., e Barros, P., Eds.; Engebook/Publindustria, Edições Técnicas, Lda: Lisboa, Portugal, 1988; ISBN 978-989-723-118-6.

40. Kramling, T.E.; Singleton, V.L. An Estimate of the Nonflavonoid Phenols in Wines. *Am. J. Enol. Vitic.* **1969**, *20*, 86–92.

41. Ribéreau-Gayon, P.; Glories, Y.; Maujean, A.; Dubourdieu, D. *Handbook of Enology-Volume 2. The Chemistry of Wine Stabilization and Treatments*, 2nd ed.; John Wiley & Sons, Inc: Hoboken, NJ, USA, 2021; Volume 2, ISBN 9780470010396.

42. Somers, T.C.; Evans, M.E. Spectral Evaluation of Young Red Wines: Anthocyanin Equilibria, Total Phenolics, Free and Molecular SO_2, "Chemical Age". *J. Sci. Food Agric.* **1977**, *28*, 279–287. [CrossRef]

43. Ribéreau-Gayon, P.; Stonestreet, E. Dosage des Tanins du Vin Rouge et Détermination de Leur Structure. *Chim. Anal.* **1966**, *48*, 188.

44. Spagna, G.; Pifferi, G.; Rangoni, C.; Mattivi, F.; Nicolinib, G.; Palmonari, R. The Stabilization of White Wines by Adsorption of Phenolic Compounds on Chitin and Chitosan. *Food Res. Int.* **1996**, *29*, 241–248. [CrossRef]

45. Schanda, J. *Colorimetry: Understanding the CIE System*; John Wiley & Sons, Inc: Hoboken, NJ, USA, 2007; ISBN 978-0-470-04904-4.

46. Jorge, N.; Teixeira, A.R.; Matos, C.C.; Lucas, M.S.; Peres, J.A. Combination of Coagulation–Flocculation–Decantation and Ozonation Processes for Winery Wastewater Treatment. *Int. J. Environ. Res. Public Health* **2021**, *18*, 8882. [CrossRef]

47. Hojiyev, R.; Ulcay, Y.; Çelik, M.S. Development of a Clay-Polymer Compatibility Approach for Nanocomposite Applications. *Appl. Clay Sci.* **2017**, *146*, 548–556. [CrossRef]

48. Schuttlefield, J.D.; Cox, D.; Grassian, V.H. An Investigation of Water Uptake on Clays Minerals Using ATR-FTIR Spectroscopy Coupled with Quartz Crystal Microbalance Measurements. *J. Geophys. Res. Atmos.* **2007**, *112*, 1–14. [CrossRef]
49. Sevim, A.M.; Hojiyev, R.; Gül, A.; Celik, M.S. Preparation of Novel Heterogeneous Catalysts by Adsorption of a Cationic Tetrapyrrole on to Bentonite: Equilibrium, Kinetics, and Thermodynamics. *Mon. Für Chem.-Chem. Mon.* **2012**, *143*, 385–400. [CrossRef]
50. Żymankowska-kumon, S.; Holtzer, M.; Olejnik, E.; Bobrowski, A. Influence of the Changes of the Structure of Foundry Bentonites on Their Binding Properties. *Mater. Sci.* **2012**, *18*, 57–61. [CrossRef]
51. Guimarães, V.; Teixeira, A.R.; Lucas, M.S.; Silva, A.M.T.; Peres, J.A. Pillared Interlayered Natural Clays as Heterogeneous Photocatalysts for H_2O_2-Assisted Treatment of a Winery Wastewater. *Sep. Purif. Technol.* **2019**, *228*, 115768. [CrossRef]
52. Barros, W.R.P.; Steter, J.R.; Lanza, M.R.V.; Tavares, A.C. Catalytic Activity of $Fe_{3-x}Cu_xO_4$ ($0 \leq x \leq 0.25$) Nanoparticles for the Degradation of Amaranth Food Dye by Heterogeneous Electro-Fenton Process. *Appl. Catal. B Environ.* **2016**, *180*, 434–441. [CrossRef]
53. Guimarães, V.; Lucas, M.S.; Peres, J.A. Combination of Adsorption and Heterogeneous Photo-Fenton Processes for the Treatment of Winery Wastewater. *Environ. Sci. Pollut. Res.* **2019**, *26*, 31000–31013. [CrossRef]
54. Putra, E.K.; Pranowo, R.; Sunarsob, J.; Indraswati, N.; Ismadji, S. Performance of Activated Carbon and Bentonite for Adsorption of Amoxicillin from Wastewater: Mechanisms, Isotherms and Kinetics. *Water Res.* **2009**, *43*, 2419–2430. [CrossRef] [PubMed]
55. Bergaya, F.; Theng, B.K.G.; Lagaly, G. *Handbook of Clay Science, Volume 1*; Elsevier: Amsterdam, The Netherlands, 2006; ISBN 9780080457635.
56. Guimarães, V.; Rodríguez-Castellón, E.; Algarra, M.; Rocha, F.; Bobos, I. Influence of pH, Layer Charge Location and Crystal Thickness Distribution on U(VI) Sorption onto Heterogeneous Dioctahedral Smectite. *J. Hazard. Mater.* **2016**, *317*, 246–258. [CrossRef] [PubMed]
57. Benna, M.; Magnin, A.; Bergaya, F. Effect of pH on Rheological Properties of Purified Sodium Bentonite Suspensions. *J. Colloid Interface Sci.* **1999**, *218*, 442–455. [CrossRef] [PubMed]
58. Sharma, P.; Borah, D.J.; Das, P.; Das, M.R. Cationic and Anionic Dye Removal from Aqueous Solution Using Montmorillonite Clay: Evaluation of Adsorption Parameters and Mechanism. *Desalin. Water Treat.* **2016**, *57*, 8372–8388. [CrossRef]
59. Zonfrilli, F.; Germanà, S.; Guida, V.; Italia, G. Thermal Stability of Dry Detergent Formulation Containing Sodium Percarbonate. *Chem. Eng. Trans.* **2009**, *17*, 705–710. [CrossRef]
60. Rodríguez-Chueca, J.; Amor, C.; Mota, J.; Lucas, M.S.; Peres, J.A. Oxidation of Winery Wastewater by Sulphate Radicals: Catalytic and Solar Photocatalytic Activations. *Environ. Sci. Pollut. Res.* **2017**, *24*, 22414–22426. [CrossRef]
61. Rodríguez-Chueca, J.; Amor, C.; Silva, T.; Dionysiou, D.D.; Li, G.; Lucas, M.S.; Peres, J.A. Treatment of Winery Wastewater by Sulphate Radicals: HSO_5^-/Transition Metal/UV-A LEDs. *Chem. Eng. J.* **2017**, *310*, 473–483. [CrossRef]
62. Deng, Y.; Ezyske, C.M. Sulfate Radical-Advanced Oxidation Process (SR-AOP) for Simultaneous Removal of Refractory Organic Contaminants and Ammonia in Landfill Leachate. *Water Res.* **2011**, *5*, 6189–6194. [CrossRef]
63. Hilles, A.H.; Abu, S.S.; Hussein, R.A.; El-Sebaie, O.D.; Arafa, A.I. Performance of Combined Sodium Persulfate/H_2O_2 Based Advanced Oxidation Process in Stabilized Land Fi Ll Leachate Treatment. *J. Environ. Manag.* **2016**, *166*, 493–498. [CrossRef] [PubMed]
64. Huie, R.E.; Clifton, C.L.; Neta, P. Electron Transfer Reaction Rates and Equilibria of the Carbonate and Sulfate Radical Anions. *Int. J. Radiat. Appl. Instrum. Part C Radiat. Phys. Chem.* **1991**, *38*, 477–481. [CrossRef]
65. Han, D.; Wan, J.; Ma, Y.; Wang, Y.; Huang, M.; Chen, Y.; Li, D.; Guan, Z.; Li, Y. Enhanced Decolorization of Orange G in a Fe (II)-EDDS Activated Persulfate Process by Accelerating the Regeneration of Ferrous Iron with Hydroxylamine. *Chem. Eng. J.* **2014**, *256*, 316–323. [CrossRef]
66. Hilles, A.H.; Abu, S.S.; Hussein, R.A.; Arafa, A.I.; El-sebaie, O.D. Effect of Persulfate and Persulfate/H2O2 on Biodegradability of an Anaerobic Stabilized Landfill Leachate. *Waste Manag.* **2015**, *44*, 172–177. [CrossRef] [PubMed]
67. Candia-Onfray, C.; Espinoza, N.; da Silva, E.B.S.; Toledo-Neira, C.; Espinoza, L.C.; Santander, R.; García, V.; Salazar, R. Treatment of Winery Wastewater by Anodic Oxidation Using BDD Electrode. *Chemosphere* **2018**, *206*, 709–717. [CrossRef] [PubMed]
68. Furman, O.S.; Teel, A.L.; Ahmad, M.; Merker, M.C.; Watts, R.J. Effect of Basicity on Persulfate Reactivity. *J. Environ. Eng.* **2011**, *137*, 241–247. [CrossRef]
69. Yang, Y.; Pignatello, J.J.; Ma, J.; Mitch, W.A. Comparison of Halide Impacts on the Efficiency of Contaminant Degradation by Sulfate and Hydroxyl Radical-Based Advanced Oxidation Processes (AOPs). *Environ. Sci. Technol.* **2014**, *48*, 2344–2351. [CrossRef] [PubMed]
70. Zhao, D.; Liao, X.; Yan, X.; Huling, S.G.; Chai, T.; Tao, H. Effect and Mechanism of Persulfate Activated by Different Methods for PAHs Removal in Soil. *J. Hazard. Mater.* **2013**, *254–255*, 228–235. [CrossRef]
71. Zrinyi, N.; Pham, A.L. Oxidation of Benzoic Acid by Heat-Activated Persulfate: Effect of Temperature on Transformation Pathway and Product Distribution. *Water Res.* **2017**, *120*, 43–51. [CrossRef] [PubMed]
72. Jaafarzadeh, N.; Ghanbari, F.; Alvandi, M. Integration of Coagulation and Electro-Activated HSO_5^- to Treat Pulp and Paper Wastewater. *Sustain. Environ. Res.* **2017**, *27*, 223–229. [CrossRef]
73. Amor, C.; De Torres-Socías, E.; Peres, J.A.; Maldonado, M.I.; Oller, I.; Malato, S.; Lucas, M.S. Mature Landfill Leachate Treatment by Coagulation/Flocculation Combined with Fenton and Solar Photo-Fenton Processes. *J. Hazard. Mater.* **2015**, *286*, 261–268. [CrossRef] [PubMed]
74. Casa, R.; Annibale, A.D.Õ.; Pieruccetti, F.; Stazi, S.R.; Sermanni, G.G.; Cascio, B. Lo Reduction of the Phenolic Components in Olive-Mill Wastewater by an Enzymatic Treatment and Its Impact on Durum Wheat (Triticum Durum Desf.) Germinability. *Chemosphere* **2003**, *50*, 959–966. [CrossRef]
75. Mosse, K.P.M.; Patti, A.F.; Christen, E.W.; Cavagnaro, T.R. Winery Wastewater Inhibits Seed Germination and Vegetative Growth of Common Crop Species. *J. Hazard. Mater.* **2010**, *180*, 63–70. [CrossRef] [PubMed]

76. Rizzo, L.; Fiorentino, A.; Grassi, M.; Attanasio, D.; Guida, M. Advanced Treatment of Urban Wastewater by Sand Filtration and Graphene Adsorption for Wastewater Reuse: Effect on a Mixture of Pharmaceuticals and Toxicity. *J. Environ. Chem. Eng.* **2015**, *3*, 122–128. [CrossRef]

77. Lucas, M.S.; Peres, J.A.; Li, G. Treatment of Winery Wastewater by Ozone-Based Advanced Oxidation Processes (O_3, O_3/UV and O_3/UV/H_2O_2) in a Pilot-Scale Bubble Column Reactor and Process Economics. *Sep. Purif. Technol.* **2010**, *72*, 235–241. [CrossRef]

78. Li, L.; Sun, B. Grape and Wine Polymeric Polyphenols: Their Importance in Enology. *Crit. Rev. Food Sci. Nutr.* **2019**, *59*, 563–579. [CrossRef] [PubMed]

79. Cheynier, V.; Dueñas-Paton, M.; Salas, E.; Maury, C.; Souquet, J.; Sarni-manchado, P.; Fulcrand, H. Structure and Properties of Wine Pigments and Tannins. *Am. J. Enol. Vitic.* **2006**, *57*, 298–305. [CrossRef]